STUDY ON THE INTEGRATION OF THE CREEP LAW FROM ARTIFICIAL NEURAL NETWORK METHODOLOGY IN THE DELAYED HYDRIDE CRACKING ASSESSMENT OF THE CANDU PRESSURE TUBES

VASILE RADU, LIVIA STOICA, DENISA TOMA, VALENTIN OLARU
Institute for Nuclear Research (RATEN ICN) Piteşti, Romania
e-mail: vasile.radu@nuclear.ro

Abstract

The paper objective is to implement the creep law in the assessment of Delayed Hydride Cracking (DHC) for CANDU pressure tubes, following the process-zone methodology stated in the CAN/CSA N285.8 standard. A complex flaw has been chosen, represented by a Bearing Pad Fretting Flaw (BPFF) that contains also a Debris Fretting Flaw (DFF), for the analyses. For the stress relaxation, at the flaw tip, it is used for the first time a creep law, which has been developed at RATEN ICN, based on the artificial neural network (NN) methodology. The NN model is called Multilayer Feedforward Neural Network, and it gives an explicit relationship for the radial strain rate of the Zr-2.5%Nb pressure tube. A finite element model was implemented in specialized software, VisualFEA, to obtain the stress-strain field and the process zone methodology was run in a MATLAB environment employing specific scripts. As results, the convergent solutions are obtained after some trials for the process-zone displacements. These allow evaluating the prevention against DHC from the specified complex flaw of the CANDU pressure tubes in operation after certain effective full power hours (EFPH).

Keywords: *process zone, delayed hydride cracking, creep law, artificial neural network*

Introduction

The operating experience from the CANDU community revealed that during the normal operation of fuel channels, there is a significant probability of flaws presence due to corrosion coupled with bearing pad fretting on the inner pressure tube surface. Typical flaws found by in-service inspection on the pressure tubes, Zr-2.5%Nb alloy, are bearing pad fretting flaw (BPFF) and debris fretting flaw (DFF). These flaws may promote cracking when certain stress-temperature scenarios happen and also the equivalent hydrogen concentration exceed the terminal solid solubility limit. In that situation, the brittle phase particles of zirconium are grown inside of a pressure tube wall, and these particles are called hydrides. The cracking of the hydrides could happen during cool down or heat transients of the reactor, and the repetitive cracking process is called delayed hydride cracking (DHC). DHC is the most damaging phenomenon of the CANDU pressure tubes, Zr-2.5%Nb, the prevention against cracking requesting carefully and integrated structural integrity analyses.

Canadian Standard N285.8 which contains the procedures and methodologies to assess CANDU pressure tubes, made from Zr-2.5%Nb alloy, contain Clause 12, which states actions requested if the flaws dos not satisfy the acceptance criteria. That means a fitness-for-service should be performed on the pressure tube flaws and this must demonstrate that the structural integrity is maintained until the next planned in-service inspection.

The paper analyses a model of the complex flaw with the location of the inner surface of the CANDU pressure tube constitutes a bearing pad fretting flaw containing another small one, as debris fretting flaw at the deepest surface. For the assessment of the DHC in the pressure tubes, it is used the engineering process-zone procedure (EPZ), which is described in the Canadian Standard N285.8 [1]. For the principal stress relaxation, it is used for the first time at RATEN ICN Pitesti, the creep strain rate for CANDU pressure tubes, Zr-2.5%Nb, which has been obtained in the framework of the artificial neural network methodology.

The first chapter shortly describes the engineering process-zone procedure from [1, 2] and it is focused mainly on the process-zone displacement methodology, and how it is used to assess the DHC initiation. The main steps to solve numerical Neuber's rule, to estimate the localized creep and the stress relaxation at the flaw tip, playing the role of mechanical stress intensifier, are exposed in next chapter. The basic methodology to obtain the Multilayer Feedforward Neural Network model and how it is used to describe the radial strain rate for CANDU pressure tubes are contained in another chapter. The modelling of the complex flaw (BPFF plus DFF) located on the inner pressure tube surface and the stress-strain analyses are performed with VisualFEA software by finite element method. Final chapter contains the results and discussion.

Short description of process-zone displacement criterion

Methodology for DHC initiation by Engineering Process Zone (EPZ) is described in the Canadian Standard N285.8 [1, 2]. Model from EPZ is based on the hydrided region in front of crack as a tiny singular entity called ″process zone″.

Inside of the process zone, the stress and strain have to reach the critical values to initiate DHC. Ideally, it is considered that tensile stress in the process zone is constant, $\boldsymbol{p_H}$, and produces a displacement at flaw tip, $\mathbf{v_T}$. When hydrides density increases inside of the process zone, then $\boldsymbol{p_H}$ decrease and process zone displacement $\mathbf{v_T}$ increase. It is supposed that cohesion lost at the process zone edge corresponds to the DHC initiation and this comes if the $\mathbf{v_T}$ value reaches the critical value, $\mathbf{v_C}$. Moreover, there is a threshold value for $\boldsymbol{p_H}$, under which the hydrided region does not fracture, and this is noted as $\boldsymbol{p_C}$. Consequently, to initiate DHC two conditions should be simultaneously met:

$$v_T \geq v_C \tag{1}$$

$$p_H \geq p_C \tag{2}$$

Also, $\boldsymbol{p_C}$ parameter is defined as threshold stress for which a hydrided region at a plane surface can crack by DHC. The critical value, $\mathbf{v_C}$ is inferred with the relationship:

$$v_C = \frac{K_{IH}^2}{E' p_C} \tag{3}$$

$$E' = \frac{E}{1-\nu^2} \tag{4}$$

Here, $\boldsymbol{E}$ – Young modulus, $\boldsymbol{\upsilon}$ – Poisson coefficient, $\mathbf{K_{IH}}$ – isotherm stress intensity factor for the cracking initiation as DHC from a specific crack.

Standard CAN/CSA N285.8 mentions that the engineering process zone calculations are based on the cubic polynomial fitting of stress distribution in front of the crack. In the present paper, the stress field around the flaw region is obtained by the finite element method with VisualFEA software [3].

The calculation of process zone displacement $\mathbf{v_T}$ also includes the process zone length, $\boldsymbol{s}$. To obtain numerical values for mentioned parameters, $\mathbf{v_T}$ and $\boldsymbol{s}$, the following steps must be performed.

Step 1. Based on the stress field in the flaw front from FEA, a cubic polynomial fitting is required:

$$\sigma(x) = A_0 + A_1\left(\frac{x}{x_0}\right) + A_2\left(\frac{x}{x_0}\right)^2 + A_3\left(\frac{x}{x_0}\right)^3 \tag{5}$$

with: $\boldsymbol{A_i}$ – fitting coefficients, $\boldsymbol{x}$– length from flaw tip in the process zone, along the radial direction of the pressure tube, $\boldsymbol{x_0}$ – length used for the cubic polynomial fitting.

Step 2. Process zone length, $\boldsymbol{s}$. The process zone length uses the coefficients from the relationship and is a solution obtained from the following equation:

$$g_0 f_0 (A_0 - p_H) + g_1 f_1 A_1\left(\frac{s}{x_0}\right) + g_2 f_2 A_2\left(\frac{s}{x_0}\right)^2 + g_3 f_3 A_3\left(\frac{s}{x_0}\right)^3 = 0 \tag{6}$$

Here, $\boldsymbol{g_i}$ and $\boldsymbol{f_i}$ are coefficients and geometric factors defined in [1]. The process zone length, $\boldsymbol{s}$, is obtained after an iterative process, as described as well in [1].

Step 3. Displacement of the process zone, $\mathbf{v_T}$. After obtaining the polynomial distribution of stress, based on the finite element stress field in front of the flaw tip, the process zone displacement is obtained from the equation:

$$v_T = \frac{5.1869 \cdot s}{E'}\left(\frac{s}{x_0}\right)\left[f_1 A_1\left(\frac{h_1}{2} - \frac{g_1}{g_0}h_0\right) + f_2 A_2\left(\frac{h_2}{2} - \frac{g_2}{g_0}h_0\right)\left(\frac{s}{x_0}\right) + f_3 A_3\left(\frac{h_3}{2} - \frac{g_3}{g_0}h_0\right)\left(\frac{s}{x_0}\right)^2 \right] \tag{7}$$

Details on $\boldsymbol{h_i}$ coefficients can be found in [1].

Step 4. Evaluation of DHC prevention. The prevention against DHC is proved when the next criterion is met:

$$C_v \cdot v_T < v_C \tag{8}$$

For the $\mathbf{C_V}$ coefficient there are the following options:
- $\mathbf{C_V = 1.0}$, for stress analyses in the elastic domain;
- $\mathbf{C_V = 1.15}$, for stress analyses in the elastic-plastic domain, and considering the creep influence.

Localized creep approach and stress relaxation at flaws

When a structural component has loaded in tensile, usually the stresses around the flaw tip are higher than those in the rest of the material. Overtime will be the stress relaxation in these locations and the creep phenomenon enhances it. Therefore any assessment based on the stress values in front of the flaw tip has to consider the stress relaxation and increasing of the strain. In a previous work [4], has been developed a numerical procedure to account for the stress relaxation in front of a flaw from a CANDU pressure tube, using Neuber's rule [5, 6]. The incremental decrease in stress for an elementary Δt_n is [4]:

$$\Delta\sigma^{t_n} = \frac{-\Delta\sigma^{t_{n-1}} \cdot \varepsilon^{c_n}}{\frac{2}{E}\Delta\sigma^{t_{n-1}} + \varepsilon^{p_0} + \varepsilon^{c_n}} \tag{9}$$

where ε^{p_0} is the plastic strain at the moment $\boldsymbol{t = 0}$.

The incremental creep strain $\Delta\varepsilon^{c_n}$ is derived from the creep law:

$$\Delta\varepsilon^{c_n} = \Delta t_n \cdot \dot{\varepsilon}^c(\sigma; t) \tag{10}$$

To start the stress relaxation procedure the elastic-plastic approach, which has been mentioned above, there is a need to obtain the current status of the stress-strain field around the flaw. For this, it is necessary to combine Neuber's rule with the Ramberg-Osgood constitutive equation. Using equivalence of the deformation energy [5, 6] and Ramberg-Osgood equation [7]:

$$\sigma^e \cdot \varepsilon^e = \sigma \cdot \varepsilon \tag{11}$$

$$\frac{\varepsilon}{\varepsilon_0} = \frac{\sigma}{\sigma_0} + \alpha \cdot \left(\frac{\sigma}{\sigma_0}\right)^n \tag{12}$$

Here ε_0 is the reference strain and is usually taken as $\varepsilon_0 = \varepsilon_{0.2}$, resulting:

$$\frac{\sigma^e \cdot \varepsilon^e}{\sigma \cdot \varepsilon_{0.2}} = \frac{\sigma}{\sigma_{0.2}} + \alpha \cdot \left(\frac{\sigma}{\sigma_{0.2}}\right)^n \quad (13)$$

Also, for the elastic domain we have:

$$\varepsilon^e = \frac{\sigma^e}{E} \quad (14)$$

Then, Eq.(13) becomes:

$$\frac{(\sigma^e)^2}{\sigma \cdot E \cdot \varepsilon_{0.2}} = \frac{\sigma}{\sigma_{0.2}} + \alpha \cdot \left(\frac{\sigma}{\sigma_{0.2}}\right)^n \quad (15)$$

With elastic stress values from finite element analyses, from Eq.(15) is obtained the solution of elastic-plastic stress σ^{P_0}. In the next step, plastic deformation at the initial moment (***t = 0***) is obtained from the equation:

$$\varepsilon^{P_0} = \varepsilon_{0.2} \cdot \frac{\sigma^{P_0}}{\sigma_{0.2}} + \alpha \cdot E \cdot \varepsilon_{0.2} \left(\frac{\sigma}{\sigma_{0.2}}\right)^n \quad (16)$$

With solution for σ^{P_0} and ε^{P_0}, we can move on to the iterative calculation based on the adequate strain rate creep law.

Creep approach modelling for CANDU pressure tube in the artificial neural network modelling

For the stress relaxation, at the flaw tip, in the present paper, it is used for the first time a creep law, which has been developed at RATEN ICN [8]. The creep law in terms of radial strain rate of CANDU pressure tube used the framework of the artificial neural network (NN) methodology [9-11]. The NN model is called Multilayer Feedforward Neural Network (MFNN), and it gives an explicit relationship for the radial strain rate of Zr-2.5%Nb pressure tube, as a function of various input parameters. Fig. 1 displays the MFNN model with two hidden layers, which uses transfer functions *tansig* for the hidden layer and *purelin* for the output layer that are defined in [12].

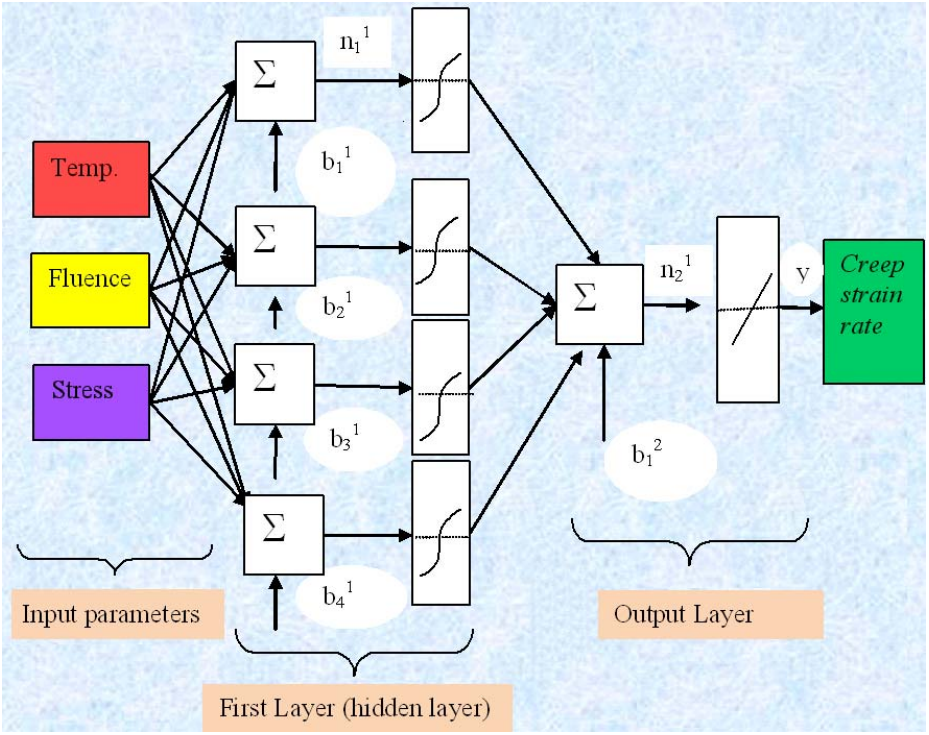


Fig.1. MFNN model with two layers used for the analysis

After optimization of the MFNN in Matlab environment [12], it was obtained a stand-alone function describing radial strain rate for CANDU pressure tubes, in the following form (from brevity reasons only first terms are displayed, but the equation contains 14 more terms):

$$F_{MFNN}(T,\sigma,\phi) = 0.248299 + \frac{0.309629}{\left(1+exp\left(7.229-0.445T+0.426\phi-3.409\sigma\right)\right)} + \ldots \quad (17)$$

Here: $F_{MFNN}(T,\sigma,\phi)$ is the radial creep strain rate (x10^{-6} h^{-1}), ***T*** is the temperature (K), ϕ is fluence (x10^{25} n/m^2), and σ is hoop stress (MPa). Eq.(17) is used in Eq.(10) of the iterative process to obtain the stress relaxation at the flaw tip after a certain period, which is expressed as effective full power hours (EFPH).

Complex flaw model and the stress analyses

Dimensional characteristics and mechanical properties for CANDU pressure tube, Zr-2.5%Nb alloy, were extracted from Canadian Standard CAN/CSA N285.8 [1]: Inner radius $R_i = 52.0$, wall thickness $t = 4.0\,mm$, Young modulus $E = 91.7\,GPa$, Poisson coefficient $\nu = 0.40$. Yield stress and ultimate tensile strength are $\sigma_{0.2} = 642\,MPa$, respectively $\sigma_{UTS} = 647.5\,MPa$ at 300 °C.

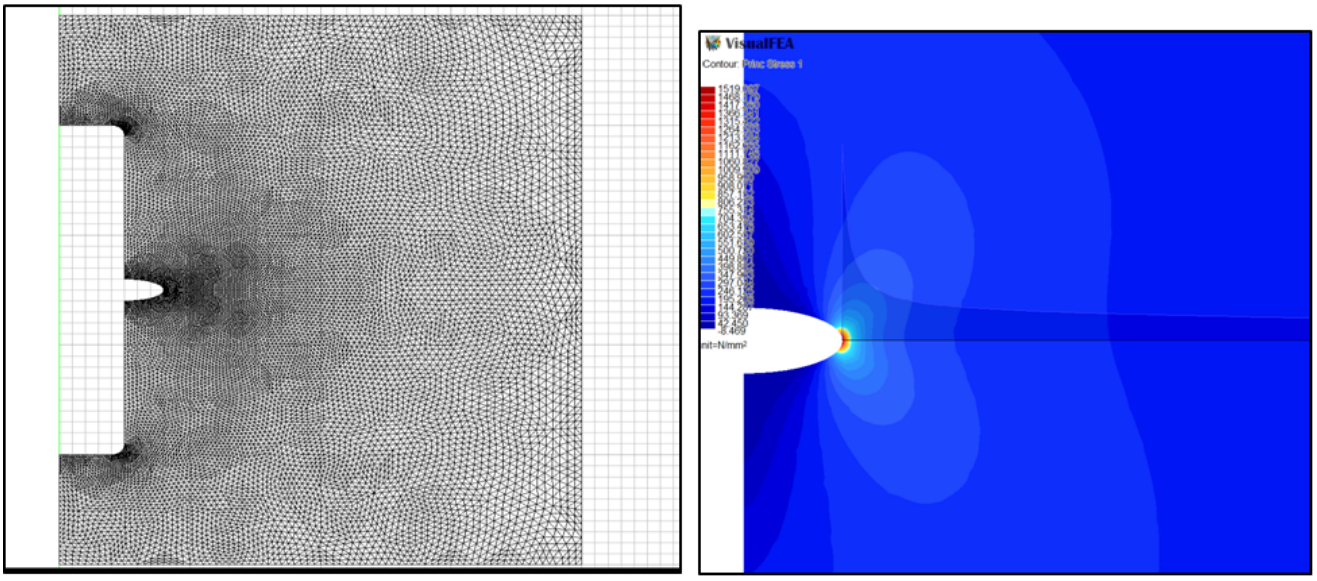
The loading condition is extracted from the operation condition of the CANDU fuel channel in the cool-down transients [13]. The stress scenario starts at an inner pressure of 10.0 MPa, and a temperature around 300 °C. Also, we consider an equivalent hydrogen concentration of 30 ppm, which means that inside the pressure tube body could be present brittle hydride platelets. The hoop nominal stress in the wall is around 140.8 MPa, and this value is considered in the finite element analyses.

A flaw complex model constitutes a bearing pad fretting flaw as a primary flaw and debris fretting flaw as a secondary flaw (BPFF plus DFF). DFF model is characterised by a flaw depth of 0.30 mm, and a root radius of 0.10 mm. For the whole complex flaw, the total depth is around 0.80 mm. For the pre and post-processing of the model with a finite element method is used computer code VisualFEA [3].

The algorithm to obtain the stress relaxation after creep, used in the present paper is:

1) The elastic stress analyses are done with VisualFEA computer code, for the complex flaw described above;
2) The principal stress values are extracted and with Neuber's rule combined with Ramberg – Osgood relationship the current stress values are obtained;
3) The plastic deformation at initial moment is inferred;
4) Start to creep analyses, $\Delta\varepsilon^{c_n} = \Delta t_n \cdot \dot{\varepsilon}^c(\sigma;t)$, for a given increment of time, Δt_n;
5) The decrease in stress $\Delta\sigma^{t_n}$ is obtained induced by the incremental increase $\Delta\varepsilon^{c_n}$;
6) The total deformation is inferred until the current step;
7) Iterate steps from 4th to 6th, until the specified creep time is reached;
8) This result in principal stress relaxation as $\sigma_1 = \sigma_1(t)$ and total plastic deformation due to the localized creep at flaw tip.

Fig. 2 displayed the flaw mesh (Fig. 2a) and the principal stress around the secondary flaw (Fig. 2b).



a) b)

Fig.2. Complex flaw model in VisualFEA (a), and the principal stress around the secondary flaw, with superimposed principal stress dependence along with the distance from flaw tip (b)

The process zone calculations are based on the stress values very close to the flaw tip, where the decrease of stress is very sharp (Fig.2). Therefore, the stress values are extracted from VisualFEA post-processing data in the region of (0; 85.2) µm, near the flaw tip. This is based on the hypothesis that the process one length, ***s***, is around 85 µm.

After run elastic analysis in VisualFEA, with input parameters described before, it was possible to extract the principal stress value along with the distance from the flaw tip (Fig.3).

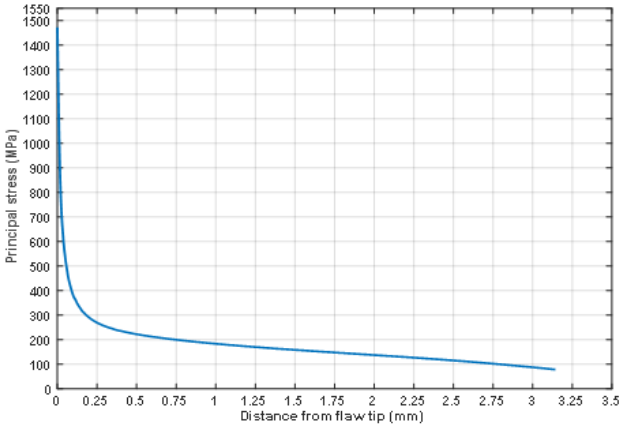


Fig.3. Principal stress variation along with the distance from flaw tip

Following the before mentioned steps of the analysis, the principal stress values are extracted and with Neuber's rule combined with Ramberg – Osgood relationship the current stress values are obtained, and variation with distance from flaw tip are displayed in Fig. 4.

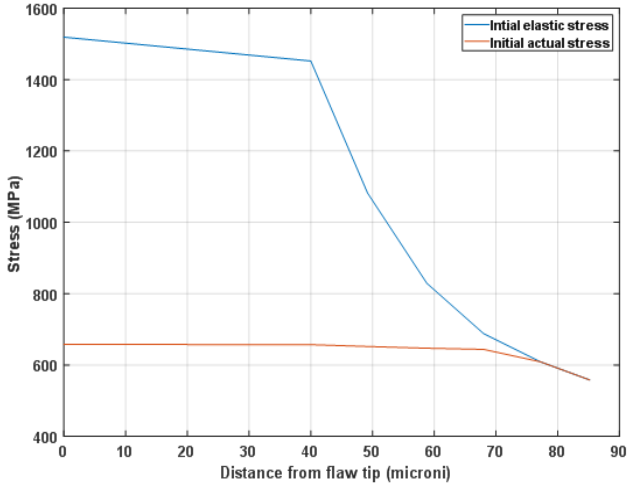


Fig.4. Initial and actual stress variation along with the distance from flaw tip

Results: Creep analyses and Process zone criterion for DHC initiation

To obtain the stress relaxation due to creep phenomenon, a period of 24 KEFPH (kilo effective power hours) was used. This period has been used at Cernavoda NPP Unit 1 as inspection interval time. The relationship for the radial strain rate given by Eq.(17), was obtained in the framework of artificial neural network methodology, at a temperature of 580K and a fast neutron flux of 2.66×10^{17} n/m^2/s.

Fig.5 displays a comparison between initial actual stress around the flaw tip, and stress after relaxation by the creep after 24 KEFPH.

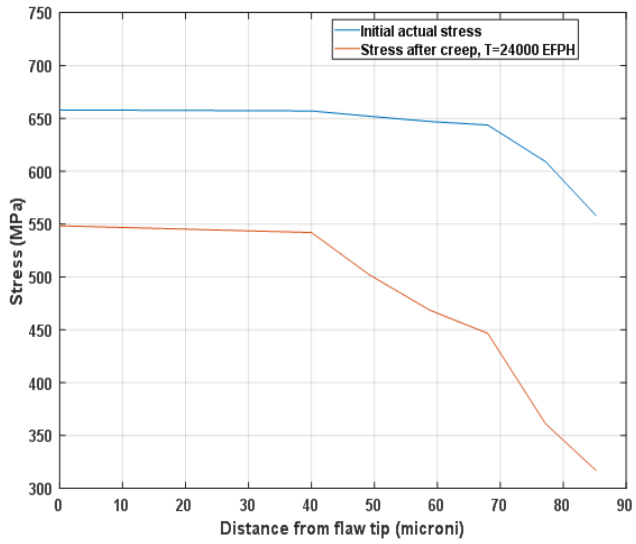


Fig.5. Stress relaxation due to the creep after 24 KEFPH at flaw tip

Based on the stress values inside of the process zone, as can be seen in Fig.5, it starts the iteration to obtain the proper process zone length, using the methodology described in Canadian Standard N285.8. Note that was created a script in the Matlab [14] environment to perform iteration trials and after a couple of runs, it is obtained the process zone length, ***s***. Inside of this process zone, a polynomial fitting of stress versus distance is realized. The accuracy of the polynomial fitting could be seen in Fig. 6, compared with the stress values after creep relaxation.

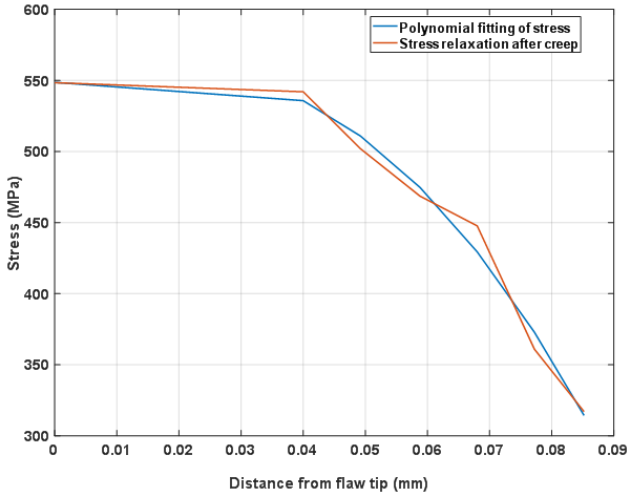


Fig.6. Polynomial fitting of stress after creep inside of the process zone

The results of the process zone analyses, after iterations in the Matlab environment, are shown in Table 1.

Table 1 Process zone criterion for DHC initiation

The characteristic parameter in the process zone	**Size**
Process zone length	$s = 85.5\ \mu m$
Critical displacement for DHC initiation	$v_c = 0.40\ \mu m$
Displacement obtained in paper at process zone edge	$v_T = 0.21\ \mu m$

Analysing the results, the criterion for DHC prevention is met: $v_C > 1.15 v_T$.

The coefficient used here C_V = 1.15 is for the stress analysis case in the elastic-plastic domain and considering the creep influence.

The conclusion of the analyses, for the complex flaw geometry on the inner surface of the CANDU pressure tube wall, is that, following stress relaxation by considering creep influence, the Delayed Hydride Cracking is not initiated. In case if the creep influence is not taken into account, then the results are different, and not conform with reality from the normal operating condition of the CANDU fuel channel.

Conclusions

The paper analyses a model of the complex flaw with the location of the inner surface of the CANDU pressure tube constitutes a bearing pad fretting flaw containing another small one, as debris fretting flaw at the deepest surface.

For the assessment of the DHC initiation in the pressure tubes, it is used the engineering process-zone procedure, which is described in the Canadian Standard N285.8. The elastic stress analyses are done with VisualFEA computer code, by the finite element method.

The principal stress values are extracted and with Neuber's rule combined with Ramberg- Osgood relationship and the current stress values are obtained. For the principal stress relaxation, it is used for the first time at RATEN ICN Pitesti, the creep strain rate for CANDU pressure tubes, Zr-2.5%Nb, which has been obtained in the framework of the artificial neural network methodology.

The conclusion of the analyses, for the complex flaw geometry on the inner surface of the CANDU pressure tube wall, is that, following stress relaxation by considering creep influence, the Delayed Hydride Cracking is not initiated. In case if the creep influence is not taken into account, then the results could be different, and not conform with reality from the normal operating condition of the CANDU fuel channel.

References

[1] *** (2005) ″CAN/CSA Standard N285.8-05: Technical requirements for in-service evaluation of zirconium alloy pressure tubes in CANDU reactors.
[2] Mok, D.H.B., Scarth, D.A. editors (2002) ″Procedures for In-Service Evaluation of Zirconium Alloy Pressure Tubes în CANDU Reactors″, CANDU Owner's Group (COG) file no. COG-02-1065.
[3] Lee, J.Y. (2007) ″VisualFEA/CBT, Computer-based Training of Finite Element Method″, Intuition Software.
[4] Radu, V., Stoica, L., Olaru, V., Nitu, A.,Ionescu, V., Mihalache, M. (2020) ″Analysis of creep-induced strains and stresses in the V notches process zone from CANDU Pressure Tubes″, *Journal of Nuclear Research and Development*, No. 19, pp. 3-6
[5] Nunez, J.E., Glinka, G. (2004) ″Analysis of non-localized creep induced strains and stresses in notches″, *Engineering Fracture Mechanics,* Vol. 71, pp.1791-1803.
[6] Nunez, J.E., Glinka, G. (2007) ″Analysis of creep-induced strains and stresses in notches subjected to a cyclic load″, *Journal of Strain Analysis*, Vol. 42, pp.361-375.
[7] Ramberg, W., Osgood, R.W. (1943) ″Description of stress-strain curves by three parameters″, *National Advisory Committee of Aeronautics*, Techn. Note 902, Nat. Bureau of Standards, Washington, DC, USA.
[8] Radu, V. (2018) ″Synthesis of the results obtained regarding the contribution of RATEN ICN to the prediction of radial deformation of the CANDU pressure tube, Zr-2.5%Nb alloy due to in-service creep under irradiation″, IAEA Vienna Contract No.17519, INR internal report, RI-11658, Institute for Nuclear Research Pitesti, Romania (in Romanian).
[9] Haykin, S. (1999) ″Neural Networks, A comprehensive foundation″ Pearson Education.
[10] Hagan, M.T., Demuth, H., Beale, M. (1996) ″Neural Network Design″, PWS Publishing Company.
[11] *** (2006) ″The Neural Network Toolbox for Use with MATLAB″, *User's Guide*, Vers.5.
[12] *** (2010) ″Matlab, Neural Network Toolbox 7″, *User's Guide*, Vers.7.
[13] *** (1998) ″Assessment and management of ageing of major nuclear power plant components important to safety: CANDU pressure tubes″, *IAEA-TECDOC-1037*.
[14] *** (2010) ″Matlab R2017b, The MathWorks″, *Inc.USA*.